Available online www.jsaer.com

***Journal of Scientific and Engineering Research*, 2023, 10(2):156-162**

Research Article

ISSN: 2394-2630
CODEN(USA): JSERBR

Numerical simulation of plasma excitation to suppress suction surface separation in low pressure turbine cascades

ZHAO xu *, ZHANG yu-xue, ZHANG yao-wen, ZHAO pei-dong

*School of Transportation and Vehicle Engineering, Shandong University of Technology, No. 266 Xincun West Road, 255049, Zibo, China

Abstract In order to investigate the effect of plasma excitation on the aerodynamic performance, separation flow control and flow field structure of low pressure turbine cascade, the exciter was loaded at different positions of the suction surface, and the flow field of low pressure turbine cascade was simulated numerically using the Transition SST transition model. The results show that the boundary layer separation on the suction surface of the cascade can be effectively suppressed at different excitation positions, and the separation point moves towards the trailing edge due to the smaller size of the separation bubble. Among them, the excitation position inside the separation bubble has a good effect on flow control. The plasma excitation reduces the total loss peak at the outlet and makes the position of the loss peak close to the pressure surface. The static pressure coefficient on the cascade surface and the shear stress on the suction surface rise sharply at the excitation position, which changes the pressure distribution on the cascade surface.

Keywords low pressure turbine, Total pressure loss, Boundary layer

1. Introduction

As one of the important components of the aeroengine, the weight of the low-pressure turbine accounts for one third of the total weight of the engine. In order to reduce the weight of the engine and improve the thrust/weight ratio of the engine, the high-load blades are gradually designed. However, the high load blade design makes the reverse pressure gradient at the rear of the suction surface of the cascade rise, and the boundary layer of the suction surface is more prone to separation [1]. In order to reduce the loss, it is necessary to control the cascade flow field.

Flow control includes passive control [2-4] and active control. As a new active flow control technology, dielectric barrier discharge plasma excitation has many advantages: 1) small size and simple structure. 2) Rapid response and low energy consumption. 3) It can adapt to different flow conditions [5]. Pescini et al. The plasma excitation effectively inhibits the expansion of the separation zone along the flow direction, and makes the separation point move downstream.

In this paper, the influence of plasma excitation on the boundary layer separation on the suction surface of low pressure turbine cascade is studied by numerical simulation.

2. Numerical simulation method

2.1. Calculate domain settings

The research object of numerical simulation is the high load low pressure turbine plane cascade T106A. Figure 1 shows the schematic diagram of the grid in the calculation domain. The grid near the end wall and cascade surface is locally densified. The number of grids in the whole calculation domain is about 2.4 million.

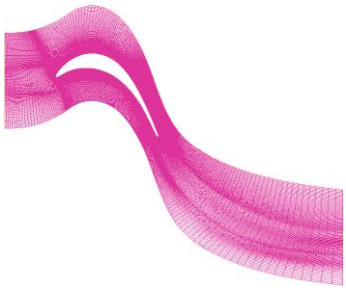

Figure 1: Calculation of domain grid maps

The transition SST turbulence model is adopted, and the Reynolds number at the cascade outlet is defined according to the isentropic expansion process under all operating conditions. The calculation formula is

$$Re_{2\text{th}} = \frac{p_2 Ma_2 C}{\mu}\sqrt{\frac{\gamma}{R}}\frac{T_0^{3/2}(T_2+110.4)}{T_2^2(T_0+110.4)} \tag{2-1}$$

Where, p_2 is the outlet static pressure; Ma_2 is the Mach number of the exit interface. The working conditions used in this numerical simulation are all Ma_2=0.4; C is the chord length of the cascade; T_0=273.16K. T_2 is the outlet static temperature during isentropic expansion, and the calculation formula is

$$T_2 = \frac{T_{t1}}{1+\frac{1}{2}(\gamma-1)Ma_2^2} \tag{2-2}$$

Where, T_{t1} is the total inlet temperature.

2.2. Plasma phenomenological model

As shown in Figure 2, the dielectric barrier discharge plasma exciter consists of the upper and lower plates, insulating dielectric and AC power supply.

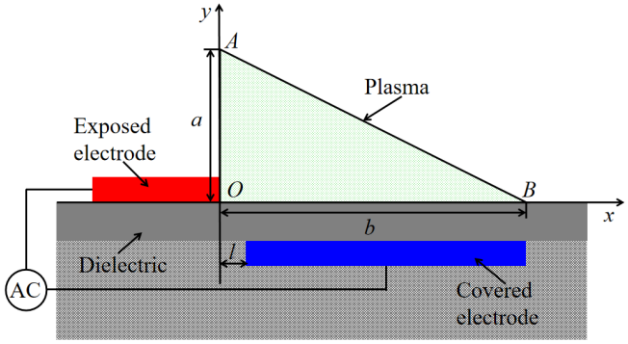

Figure 2: Sketch of plasma actuator

In this paper, the linear volumetric force model proposed by Shyy [8] is used to simulate the electric field force exerted by the strip electrode actuator on the flow field. The model assumes that the electric field force only acts in the triangle area OAB, and the electric field strength decreases linearly with the increase of the distance from the O point, The electric field intensity in the triangle OAB is $E=E_0-k_1x-k_2z$, then the electric field intensity in the x and z directions is:

$$E_x = \frac{Ek_2}{\sqrt{k_1^2 + k_2^2}} \tag{2-3}$$

$$E_z = \frac{Ek_1}{\sqrt{k_1^2 + k_2^2}} \tag{2-4}$$

Where, $k_1=(E_0-E_b)/b$ and $k_1=(E_0-E_b)/a$.

2.3. Layout scheme of plasma exciter

As shown in Figure 3, three kinds of actuator arrangement schemes are designed, namely, DBD plasma actuators are installed at 15% C_{ax} (P_1), separation point (P_2) and 15% C_{ax} (P_3) before the separation point where boundary layer separation occurs on the suction surface of the cascade.

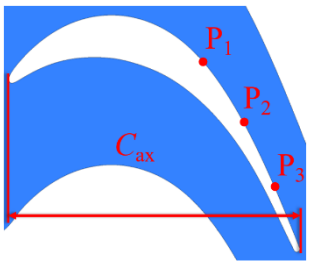

Figure 3: Layout diagram of plasma exciter

2.4. Model validation

The comparison between the numerical simulation results and the experimental results is shown in Figure 4. The results show that the numerical simulation results are in good agreement with the experimental results. The static pressure coefficient is defined as

$$C_p = \frac{p - p_2}{p_{t1} - p_2} \tag{2-5}$$

Where, p is the static pressure value of the cascade surface; p_{t1} is the total inlet pressure.

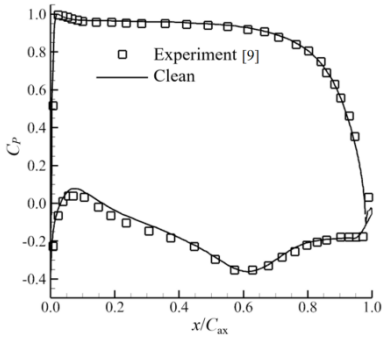

Fig. 4 Distribution of static pressure coefficient

3. Analysis of simulation results

Figure 5 shows the distribution of static pressure coefficient at different blade heights. After 80% C_{ax} of the suction surface of the cascade, a pressure platform is generated on the suction surface of the cascade, and the boundary layer is separated, resulting in separation bubbles, which increases the flow loss. In order to improve the aerodynamic performance of the low pressure turbine, the actuator arrangement scheme that can disturb the flow of the boundary layer, make the pressure platform behind 80% C_{ax} disappear, inhibit the separation of the

boundary layer, inhibit the generation of separation bubbles, and reduce the flow loss is effective. Therefore, it can be seen from the above analysis that the plasma excitation effect can effectively control the flow field of the low-pressure turbine, eliminate the pressure platform, reduce the flow loss and enhance the aerodynamic performance of the low-pressure turbine when the actuator is installed in the P_3 position. However, while eliminating the pressure platform, the lateral pressure on the suction surface and pressure surface is increased, and the secondary flow at the end of the cascade channel is enhanced.

The shear stress can reflect the separation of the boundary layer on the suction surface of the cascade. Figure 6 shows the distribution of the shear stress on the suction surface at different blade heights. Through the comparison of the distribution of the suction surface of the cascade, it can be seen that the plasma excitation effect of installing the actuator at P_3 position has better control effect on the flow of the boundary layer of the suction surface of the cascade, making more shear stresses within the axial

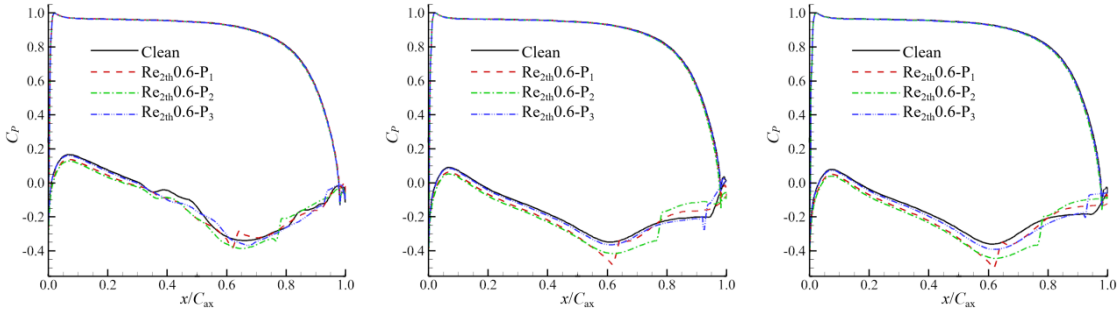

（a）z/H=0.03 （b）z/H=0.20 （c）z/H=0.50

Figure 5: Distribution of high static pressure coefficient in different leaves

chord length range at positive values, inhibiting the separation of the boundary layer and the generation of separation bubbles. Compared with the analysis results of the static pressure coefficient distribution on the suction surface of the cascade, both the static pressure coefficient distribution and the shear stress distribution on the suction surface show that the plasma excitation effect of the actuator installed at P_3 can inhibit the boundary layer separation.

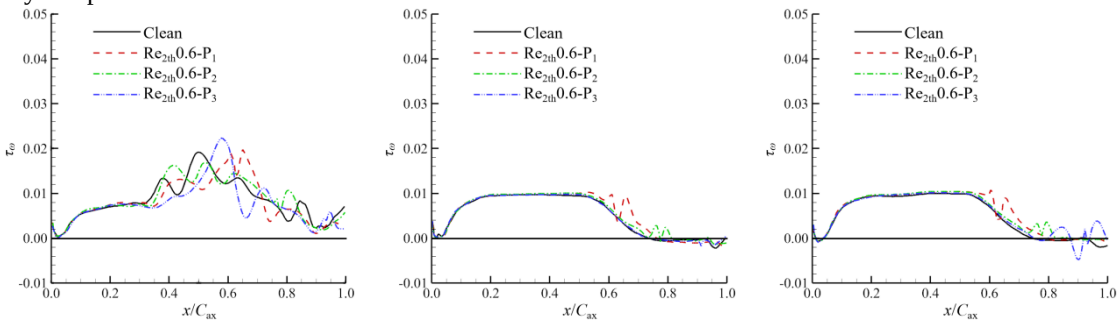

（a）z/H=0.03 （b）z/H=0.20 （c）z/H=0.50

Figure 6: Shear stress distribution on suction surface of cascade at different blade heights

Figure 7 shows the distribution of total pressure loss coefficient in different flow directions. The total pressure loss coefficient is defined as

$$\Omega = \frac{p_{t1} - p_{t2}}{p_{t1} - p_2} \tag{3-1}$$

As the flow section is closer to the outlet of the cascade channel, the mass average value of the total pressure loss coefficient on the section becomes larger and larger. And from x/C_{ax}=0.75 to x/C_{ax}=1.25, the mass average value of the total pressure loss coefficient of mass flow on the section increases sharply. When $x/C_{ax} < 1.0$, when the actuator is installed at P_3 position on each flow direction section, the total pressure loss of the average mass on the section is always greater than the other three conditions. When $0.8 < x/C_{ax} < 1.0$, the mass average total pressure loss coefficient decreases nonlinearly on the same flow direction section of $Re_{2th}0.6\text{-}P_3$, Clean,

Re_{2th}0.6-P_2 and Re_{2th}0.6-P_1 working conditions. On the flow section with x/C_{ax}=1.0, the mass average total pressure loss coefficient under Re_{2th}0.6-P_3 and Clean conditions is equal.

Figure 8 shows the distribution of the total pressure loss coefficient at the cascade outlet under four different actuator installation positions. The circumferential dimension is normalized based on the grid distance. y^*=0 is the side near the suction surface, and y^*=1 is the side near the pressure surface. When y^*< 0.15, the total pressure loss coefficient at the cascade outlet of four different actuator installation modes is equal. When 0.15 < y^* < 0.6, the spanwise average total pressure loss coefficient under Clean

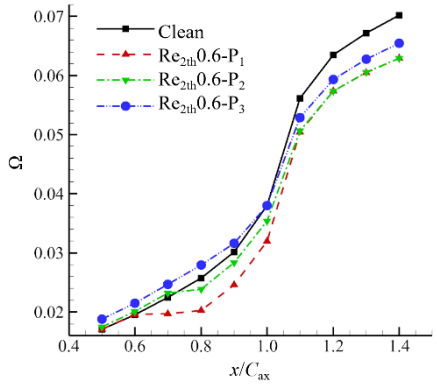

Figure 7: Distribution of total pressure loss coefficient on sections with different flow directions

condition is the largest at the same location in the circumferential direction. As the installation position of the actuator moves from the front of the separation point to the rear of the separation point, the total pressure loss gradually decreases. The total pressure loss when the actuator is installed at P_1 and P_2 is almost equal, which is between the total pressure loss when the actuator is installed at P_3 and Clean. When y^* > 0.6, the total pressure loss of the actuator installed at the same position in the circumferential direction under P_3 working condition is almost the largest, slightly higher than that under Clean working condition. The total pressure loss of the actuator installed at P_1 and P_2 is equal, which is smaller than the total pressure loss under Clean condition. It can be seen from the above analysis that when the actuator is installed at P_3 position, the total pressure loss at the cascade outlet is the smallest under the effect of plasma excitation.

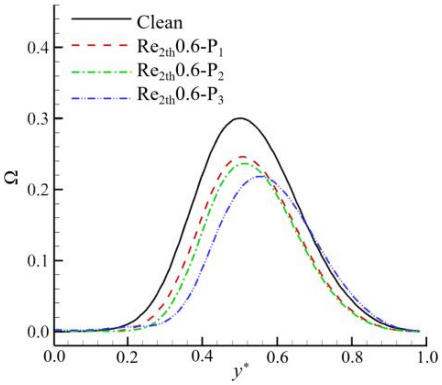

Figure 8: Distribution of total pressure loss coefficient at cascade outlet

Figure 9 shows a two-dimensional streamline diagram at 50% of the blade height. The distribution of the secondary streamline at 50% of the blade height is similar to that at 30% of the blade height. Similarly, when the actuator is installed at P3 position, the plasma excitation effect of the actuator has a better effect on the disturbance of the boundary layer flow on the suction surface of the cascade. The large separation bubble is split into two small separation bubbles under the plasma excitation effect, and the position of the separation bubble moves towards the trailing edge of the cascade.

Figure 10 shows the total pressure loss nephogram of 125% C_{ax} section. Above the blade height of z/H=0.3 and above the blade height of z/H=0.3 under four working conditions, as the installation position of the actuator moves from the front of the separation point to the rear of the separation point, the area ratio of the total pressure

loss coefficient in the range of 0.2 to 0.3 on the flow section of the cascade channel x/Max=1.25 gradually decreases, the thickness of the separation boundary layer decreases, and the total pressure loss gradually decreases. At the position of z/H=0, the total pressure

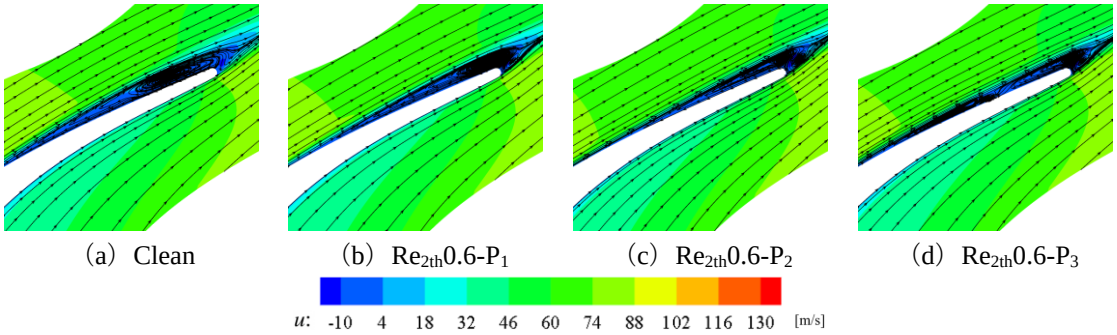

(a) Clean (b) $Re_{2th}0.6\text{-}P_1$ (c) $Re_{2th}0.6\text{-}P_2$ (d) $Re_{2th}0.6\text{-}P_3$

Figure 9: 2D streamline map and flow velocity contour

loss when the actuator is installed at P3 is lower than that at P_1 and P_2. The plasma excitation effect of the exciter at the three locations of the exciter installation has disturbed the flow field in the cascade channel and changed its original flow. Among them, the plasma excitation effect of the exciter installed at the P_3 location is better than the other two locations in reducing the total pressure loss of the flow section.

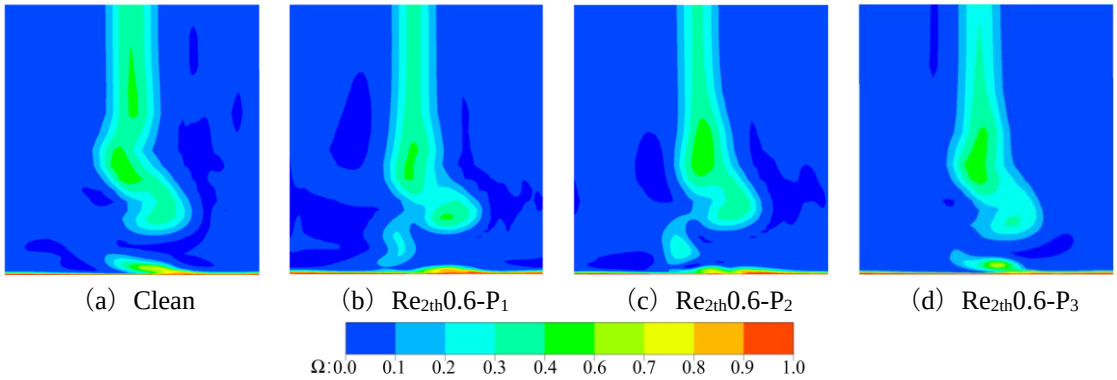

(a) Clean (b) $Re_{2th}0.6\text{-}P_1$ (c) $Re_{2th}0.6\text{-}P_2$ (d) $Re_{2th}0.6\text{-}P_3$

Figure 10: Total pressure loss contour

4. Conclusion

In this paper, T106A cascade is selected as the research object, and the influence of different excitation positions on the flow field of low pressure turbine is studied using RANS method. The main conclusions are as follows:

1) Different excitation positions can effectively inhibit the boundary layer separation on the suction surface of the cascade, and the size of the separation bubble is smaller, making the separation point move towards the trailing edge. Among them, the excitation position inside the separation bubble has a good effect on flow control.

2) The plasma excitation reduces the total loss peak at the outlet and makes the position of the loss peak close to the pressure surface.

3) The static pressure coefficient on the cascade surface and the shear stress on the suction surface rise sharply at the excitation position, which changes the pressure distribution on the cascade surface.

Reference

[1]. Hourmouziadis J. Aerodynamic Design of Low Pressure Turbines [C]// AGARD lecture series 167, 1989

[2]. Bloxham M J. A global Approach to Turbomachinery Flow Control: Loss Reduction Using Endwall Suction and Midspan Vortex Generator Jet Blowing [D]. Columbus: The Ohio State University, 2010

[3]. Benton S I, Bons J P, Sondergaard R. Secondary Flow Loss Reduction Through Blowing for a High-Lift Front-Loaded Low Pressure Turbine Cascade [J]. Journal of Turbomachinery, 2013, 135(2):021020.
[4]. Benton S I, Bernardini C, Bons J P, et al. Parametric Optimization of Unsteady End Wall Blowing on a Highly Loaded Low-Pressure Turbine [J]. Journal of Turbomachinery, 2014, 136(7): 071013
[5]. Zhang Xin, Wang Xunnian. Research progress and outlook of flow field created by dielectric barrier discharge plasma actuators driven by a sinusoidal alternating current high-voltage power. Chinese Journal of Theoretical and Applied Mechanics, 2022
[6]. Mazaheri K, Omidi J, Kiani K C. Simulation of DBD Plasma Actuator Effect on Aerodynamic Performance Improvement Using a Modified Phenomenological Model [J]. Computers & Fluids, 2016, 140: 371--384
[7]. Martinez D S, Pescini E, De Giorgi M G, et al. Plasma-Based Flow Control for Low-Pressure Turbines at Low-Reynolds-Number [J]. Aircraft Engineering and Aerospace Technology, 2017, 85(9): 671--682
[8]. Shyy, W.; Jayaraman, B.; Andersson, A.: Modeling of Glow Discharge-induced Fluid Dynamics. J. Appl. Phys. 92, 6434-6443(2002). https://doi.org/10.1063/1.1515103
[9]. Stadtmüller P . Investigation of wake-induced transition on the LP turbine cascade T106A-EIZ[C]//DFG-Verbundprojekt Fo 136/11 , Version 1.0 . Munich , Germany : University of the Armed Forces, 2001